Mon. Not. R. astr. Soc. (1992) **258,** 225–240

An observational study of the eclipsing nova-like variable BH Lyncis (≡ PG 0818 + 513)

V. S. Dhillon,[1] D. H. P. Jones,[2] T. R. Marsh[3] and R. C. Smith[1]

[1] *Astronomy Centre, Physics and Astronomy Division, University of Sussex, Falmer, Brighton BN1 9QH*
[2] *Royal Greenwich Observatory, Madingley Road, Cambridge CB3 0EZ*
[3] *Department of Astrophysics, Nuclear Physics Building, Keble Road, Oxford OX1 3RH*

Accepted 1992 March 6. Received 1992 March 6; in original form 1992 January 9

SUMMARY

We present photometric and spectroscopic observations of the nova-like variable BH Lyn. The continuum and line light curves exhibit deep eclipses which recur with a period of 3.74 hr. The spectra have single-peaked Balmer and He I emission lines which, due to the absorption of low-velocity emission, exhibit a double-peaked structure near the inferior conjunction of the emission-line source. The high-excitation lines of He II λ4686 Å and C III/N III λλ4640–4650 Å are very weak. Radial velocity measurements show large phase shifts in all the emission lines. We construct light-centre and Doppler maps of the system which suggest that the line emission is largely non-disc in origin; for this reason we do not present a full system parameter determination.

We compare and contrast BH Lyn with a number of other eclipsing nova-like variables; namely, V1315 Aql, SW Sex, DW UMa and PG 0027 + 260. The objects show basically the same behaviour, and we therefore conclude that the emission lines must be produced by a similar (unknown) mechanism. The few differences that are exhibited by BH Lyn can be attributed to the fact that the major part of our data was obtained during a temporary period of low mass transfer rate.

Key words: binaries: eclipsing – binaries: spectroscopic – stars: individual: BH Lyn – novae, cataclysmic variables.

1 INTRODUCTION

Nova-like stars are generally defined as cataclysmic variables which have never been observed to undergo dwarf nova type outbursts. Such a crude definition encompasses a wide variety of different objects which are usually categorized into three subclasses: the *magnetic variables* (such as AM Her), the *anti-dwarf novae* (such as VY Scl) and the *UX UMa stars* (see, for example, Wade & Ward 1985). A fourth subclass, the so-called *SW Sex stars* (Thorstensen *et al.* 1991b) or *quiescent novae* (Vogt 1989; Dhillon 1990), has recently appeared in the astronomical literature. These objects, of which there exist five well-studied systems (SW Sex: Honeycutt, Schlegel & Kaitchuck 1986; DW UMa: Shafter, Hessman & Zhang 1988; V1315 Aql: Dhillon, Marsh & Jones 1991; PG 0027 + 260: Thorstensen *et al.* 1991b; BH Lyn: Thorstensen, Davis & Ringwald 1991a), show a number of remarkable similarities: all five objects are eclipsing systems with orbital periods lying in the range 3.24–3.74 hr; all five objects exhibit single-peaked Balmer and He I emission lines which remain largely unobscured during primary eclipse and show strong absorption features around the inferior conjunction of the emission-line source; all five objects show single-peaked high-excitation emission lines which are eclipsed by the primary; and all five objects show radial velocity curves with significant phase shifts relative to photometric conjunction. To date, no detailed theoretical model has been able to satisfy these observational constraints (see Dhillon *et al.* 1991) and therefore we feel it is premature to create a new class for these objects (since, for example, we have no direct evidence that they actually are novae in quiescence, or that they are not just the highest inclination counterparts of UX UMa-type systems). For this reason, we shall refer to these objects as *eclipsing nova-like variables.*

BH Lyn (≡ PG 0818 + 513, Kazarovets & Samus 1990) was one of 22 cataclysmic variables discovered by their UV excesses in photographs obtained for the Palomar–Green (PG) survey (Green, Schmidt & Liebert 1986). Follow-up spectroscopic observations of this $B \sim 15.5$ mag object by

Green *et al.* (1982) revealed a high-excitation emission-line spectrum, very similar to the spectra observed in old novae. The eclipsing nature of BH Lyn was first suspected by Andronov (1986), proved by Richter (1989), and later refined by Andronov *et al.* (1989), who determined the binary period at 3.74 hr and, by virtue of its light curve, classified BH Lyn as a nova-like variable similar to DW UMa. It was this comparison, later confirmed by the spectroscopic study of Thorstensen *et al.* (1991a), that prompted our detailed observational study of BH Lyn, which we observed as part of our survey of eclipsing nova-like variables. The initial aims and results of the survey for V1315 Aql, SW Sex and DW UMa have been reported by Dhillon *et al.* (1991) and Dhillon (1990). In this paper we report on the survey results for BH Lyn.

2 THE OBSERVATIONS AND THEIR REDUCTION

2.1 Photometry

We observed BH Lyn on the night of 1990 January 12/13 with the 1-m Jacobus Kapteyn Telescope (JKT) at the Roque de los Muchachos Observatory on La Palma. The data covered ~1.1 orbits and consisted of 166 exposures taken every 60 s (~0.007 in phase, with ~30 s dead-time for the dumping of data). The observations were made in the Kron–Cousins *R* band with a GEC P8603 CCD chip, pixel size $22 \times 22\ \mu m^2$ ($\equiv 0.3 \times 0.3$ arcsec^2). The individual images were freed from bias and then flat-fielded from an image of the dawn sky. The brightness of each image was found from the total signal within a circle of 14 pixels diameter (4.2 arcsec) from which the sky signal in a surrounding annulus had been subtracted. Unfortunately, we were unable to correct for the effects of atmospheric extinction since there was no bright comparison star in the field of view, and we therefore had to assume an average extinction value for the entire night. Given that the night was photometric and the zenith distance of BH Lyn was never greater than ~30°, we estimate that the error introduced by ignoring extinction is approximately 0.02 mag. The observations were placed on an absolute flux scale by using observations of the standard star SA97-346 (Landolt 1983) taken immediately before the run. We estimate that the absolute photometry is accurate to approximately 1 mJy; the relative photometry to approximately 0.04 mag.

2.2 Spectroscopy

On the nights of 1990 January 12/13, 14/15 and 17/18, a total of 241 spectra were obtained with the 2.5-m Isaac Newton Telescope (INT) on La Palma. The exposures were either 120 or 180 s long, with about 9 s dead-time for the dumping of data. The Intermediate Dispersion Spectrograph (IDS), the Image Photon Counting System (IPCS) detector with a camera format of 2048×130 pixels, and a grating of 1200 line mm^{-1} gave a wavelength coverage of approximately $\lambda\lambda$4025–5050 Å at 1-Å ($\simeq 75$ km s^{-1}) resolution. We were able to correct for slit losses by placing a nearby comparison star on the 140×1.1 arcsec^2 slit and obtaining a photometric spectrum of the comparison star taken through a wide (8 arcsec) slit. Comparison arc spectra were taken every 30–40 min to calibrate instrumental flexure and stability (the maximum wavelength drift during the run due to spectrograph flexing was ~0.5 Å). We also took two spectra of the flux standard PG 0823+546 (Massey *et al.* 1988) to correct the instrumental wavelength response. A full journal of the spectroscopic observations is given in Table 1.

The first step in the data reduction was the preparation of a 'balance frame' from the tungsten lamp flat-fields, which we used to correct for medium-scale sensitivity variations of the detector; the large-scale variations were removed using the standard star while the small-scale variations were removed by the IPCS scanning coils (Jorden & Fordham 1986). The sky was subtracted by fitting third-order polynomials in the spatial direction to the sky regions on either side of the object. The data were then summed across the stellar profile to give a raw spectrum for the target star. The same procedure was applied to all the data frames. Two sets of arc spectra were extracted from each frame, one from the same location on the detector as BH Lyn and the other from the same location as the comparison star. The wavelength scale for each spectrum was interpolated from the wavelength scales of two neighbouring arc spectra. The root-mean-square (rms) scatter of the sixth-order polynomial fits to the arc lines was always <0.1 Å.

Our final procedure was to correct for instrumental response and slit losses in order to obtain absolute fluxes. Tabulated absolute fluxes and a polynomial fit to the continuum of the spectrophotometric standard star data were used to remove the variations of instrumental response with wavelength from both the object and comparison star spectra. The slit-loss correction was then applied by dividing the target spectra by polynomial fits to the continua of the corresponding comparison star spectra, and multiplying by a polynomial fit to the continuum of the wide-slit photometric spectrum of the same comparison star.

In addition to the data obtained in 1990 January, we also took five blue and five red spectra of BH Lyn on the night of 1991 April 30/May 1 using the ISIS triple-spectrograph on the 4.2-m William Herschel Telescope (WHT) on La Palma. A dichroic was used to split the beam by reflecting blue light through a 90° angle into the ISIS blue arm, while transmitting

Table 1. Journal of spectroscopic observations of BH Lyn.

Observation Date	1990 January 12/13	1990 January 14/15	1990 January 17/18	1991 April 30/May 1
Number of Spectra	133	34	74	10
Exposure Time (s)	120	180	180	500
Phase Coverage (cycles)	4645.32–4647.17	4659.10–4660.12	4677.59–4678.75	7679.929–7680.130
Seeing (mean)	1.2	1.1	1.6	Not Available
Photometric Conditions	Yes	No	Yes	Not Available
Flux Standard	PG 0823+546	Not Observed	PG 0823+546	HD 84937
Wide Slit Comparison	Observed	Not Observed	Observed	Not Observed

the red light into the red arm. On the blue arm we used a large-format (1280 × 1180 pixels) EEV P88300 CCD chip together with a grating of 158 line mm^{-1} to give a wavelength coverage of approximately $\lambda\lambda$ 3000–6400 Å at ~ 7-Å resolution. On the red arm we used a large-format (800 × 1180 pixels) EEV P88200 CCD chip together with a grating of 158 line mm^{-1} to give a wavelength coverage of approximately $\lambda\lambda$ 5800–9000 Å at ~ 7-Å resolution. The exposures were all 500 s long. We observed the spectrophotometric standard star HD 84937 (Oke & Gunn 1983) in order to flux calibrate the spectra and remove the telluric absorption features. However, we were unable to correct for slit losses, since no comparison star was placed on the 0.86-arcsec slit.

The raw data were first debiased and then flat-fielded by dividing each frame by a normalized flat-field (created by dividing each pixel in the debiased flat-field by the mean number of counts over the whole flat-field). The sky subtraction and spectrum extraction followed the procedure described above for the INT data. Given the total absence of arc lines in the blue half of the detector, the wavelength calibration of the blue spectra proved to be difficult. A second-order polynomial fit was therefore used in order to minimize the error in the unconstrained regions. This gave a typical rms scatter of ~ 0.5 Å. The wavelength calibration of the red spectra was better constrained and the rms scatter of the third-order polynomial fits to the arc lines was ~ 0.1 Å. The flux star was used to convert counts per second into mJy and also to correct for atmospheric absorption (following the method outlined by Marsh 1990). The final procedure was to remove by hand a total of eight cosmic rays from the 10 spectra.

3 RESULTS

3.1 Photometry

3.1.1 The ephemeris

We observed a total of three eclipses of BH Lyn. The first eclipse was observed on 1990 January 12/13 and was observed simultaneously by the JKT and INT. The second and third eclipses were observed on 1990 January 12/13 and 17/18, respectively, and were observed only with the INT. Note that we did observe through eclipse on the nights of 1990 January 14/15 and 1991 April 30/May 1, but calibration observations and poor time resolution, respectively, resulted in eclipse light curves which could not be used for ephemeris purposes. In order to derive an ephemeris for BH Lyn we fitted a parabola by least squares to the single JKT eclipse minimum and the two later INT eclipse minima (derived from the light curves of the continuum, see Section 3.2.3). These three eclipse timings, combined with the 11 timings measured by Andronov *et al.* (1989), yield the following ephemeris:

$$T_{\text{mid-eclipse}} = \text{HJD } 2\,447\,180.3369 + 0.15587507\,E. \pm 0.0002 \pm 0.00000006 \quad (1)$$

The errors in the ephemeris have been derived using the errors given by Andronov *et al.* (1989) and assuming an error of 0.001 d in our three eclipse measurements. The differences between the observed and calculated times of mid-eclipse are given in Table 2; given the distribution of eclipse timings it is impossible to say whether there is any indication of a change in the period of BH Lyn over the ~ 26-yr baseline of available eclipse timings.

3.1.2 The light curve

The JKT observations are plotted in Fig. 1 as a function of phase, following equation (1). The light curve of BH Lyn is similar to many other eclipsing nova-like variables (e.g. V1315 Aql: Downes *et al.* 1986; Dhillon *et al.* 1991; DW UMa: Shafter *et al.* 1988; SW Sex: Penning *et al.* 1984), exhibiting a symmetrical eclipse which is 2.1 mag deep (in the *R* band) and lasts for approximately 30 min. There appears to be no significant evidence for an orbital hump associated with the changing aspect of the bright-spot, although it is conceivable that the slight rise in brightness towards the end of the binary cycle is due to this effect (see Section 3.2.3 for a more detailed discussion of this feature). The flickering visible in the light curve is typically associated with emission either from the bright-spot or the inner disc. It seems likely that flickering is also responsible for the appearance of a

Table 2. Eclipse observations of BH Lyn. The differences between the observed and calculated times of mid-eclipse are given by $O-C$. The first 11 eclipse timings have been reproduced from Andronov *et al.* (1989).

HJD (mid-eclipse) (2,400,000+)	Cycle Number (E)	O − C (s)
38893.4036.....	−53164	+756.53
45758.2873.....	−9123	−115.60
47180.3363.....	0	−49.04
47180.4922.....	1	−46.89
47203.2505.....	147	−0.20
47203.4064.....	148	+1.95
47592.3150	2643	+28.70
47592.4709.....	2644	+30.86
47643.2843.....	2970	−130.85
47643.4402.....	2971	−128.69
47664.3275.....	3105	−125.14
47904.5340.....	4646	+137.55
47904.6912.....	4647	+250.33
47909.5217.....	4678	+109.54

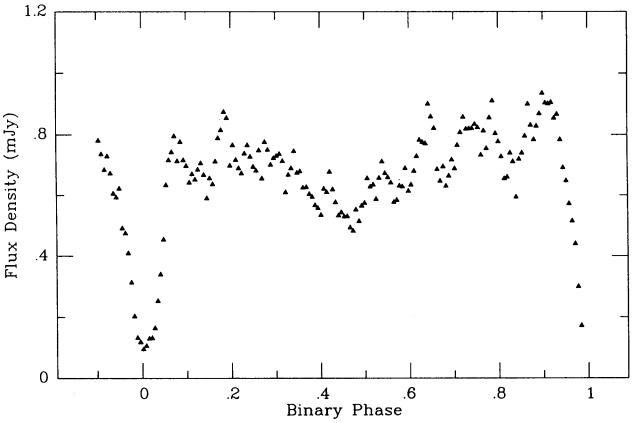

Figure 1. Light curve of BH Lyn in the *R* band.

secondary eclipse at phase 0.5, since the residual flux at phase 0 places an upper limit of 0.1 mJy for the flux from the secondary star and the eclipse at phase 0.5 appears to be ~0.2 mJy deep.

3.1.3 *Binary inclination*

By considering the geometry of a point eclipse by a spherical body, it is possible to determine the inclination, i, of a binary system using the relation

$$(R_2/a)^2 = \sin^2(\pi\Delta\phi_{1/2}) + \cos^2(\pi\Delta\phi_{1/2})\cos^2 i, \quad (2)$$

where R_2/a is defined as the volume radius of the secondary star and can be expressed solely as a function of mass ratio (Eggleton 1983). $\Delta\phi_{1/2}$ is the mean phase *full-width* of eclipse at *half* the out-of-eclipse intensity, which from the three eclipses of BH Lyn was measured to be $\Delta\phi_{1/2} = 0.081 \pm 0.006$. The solid curves in Fig. 2 show the q–i relations for this eclipse width and its error, calculated using equation (2). The dashed curve in Fig. 2 shows the results of an exact computation for $\Delta\phi_{1/2} = 0.081$, using a Roche lobe simulation similar to that of Horne, Lanning & Gomer (1982). By taking a representative value for the mass ratio of BH Lyn of $q = 0.41 \pm 0.26$ (see Section 3.2.5), we find an inclination of $i = (79.8 \pm 5.0)°$, in good agreement with the more sophisticated computation, which gives an inclination of $i = 81°.0$.

3.1.4 *Accretion disc radius*

The mean phase *half-width* of eclipse at *maximum* intensity (i.e. timing the first and last contacts of eclipse and dividing by 2) from the three INT eclipses was measured to be $\Delta\phi = 0.07 \pm 0.02$. This is effectively in the B band; the width of the R-band JKT eclipse is $\Delta\phi = 0.08 \pm 0.02$. Using these eclipse widths it is possible to determine the radius of the accretion disc, R_D, in BH Lyn through the geometric relation

$$R_D = a \sin i \sin(2\pi\Delta\phi) - R_C, \quad (3)$$

where the half-chord on the secondary, R_C, is known in terms of i and R_2/a (see, for example, Dhillon *et al.* 1991 for details).

Fig. 3 shows a plot of the disc radius versus mass ratio. The curve was produced by determining the inclination for each mass ratio using equation (2) (assuming $\Delta\phi_{1/2} = 0.081$) and then calculating the disc radius for this inclination and mass ratio (assuming $\Delta\phi = 0.07 \pm 0.02$) using equation (3). The dashed curves represent solutions where $R_D < R_C$, i.e. solutions where we would expect to see a total (flat-bottomed) eclipse. The solid curve represents solutions where $R_D > R_C$, i.e. solutions where we would expect to see a partial (round-bottomed) eclipse. Clearly, the eclipses exhibited by BH Lyn are on the verge of being total, an inference which is supported by the morphology of the eclipse light curves at different wavelengths; the ~B-band

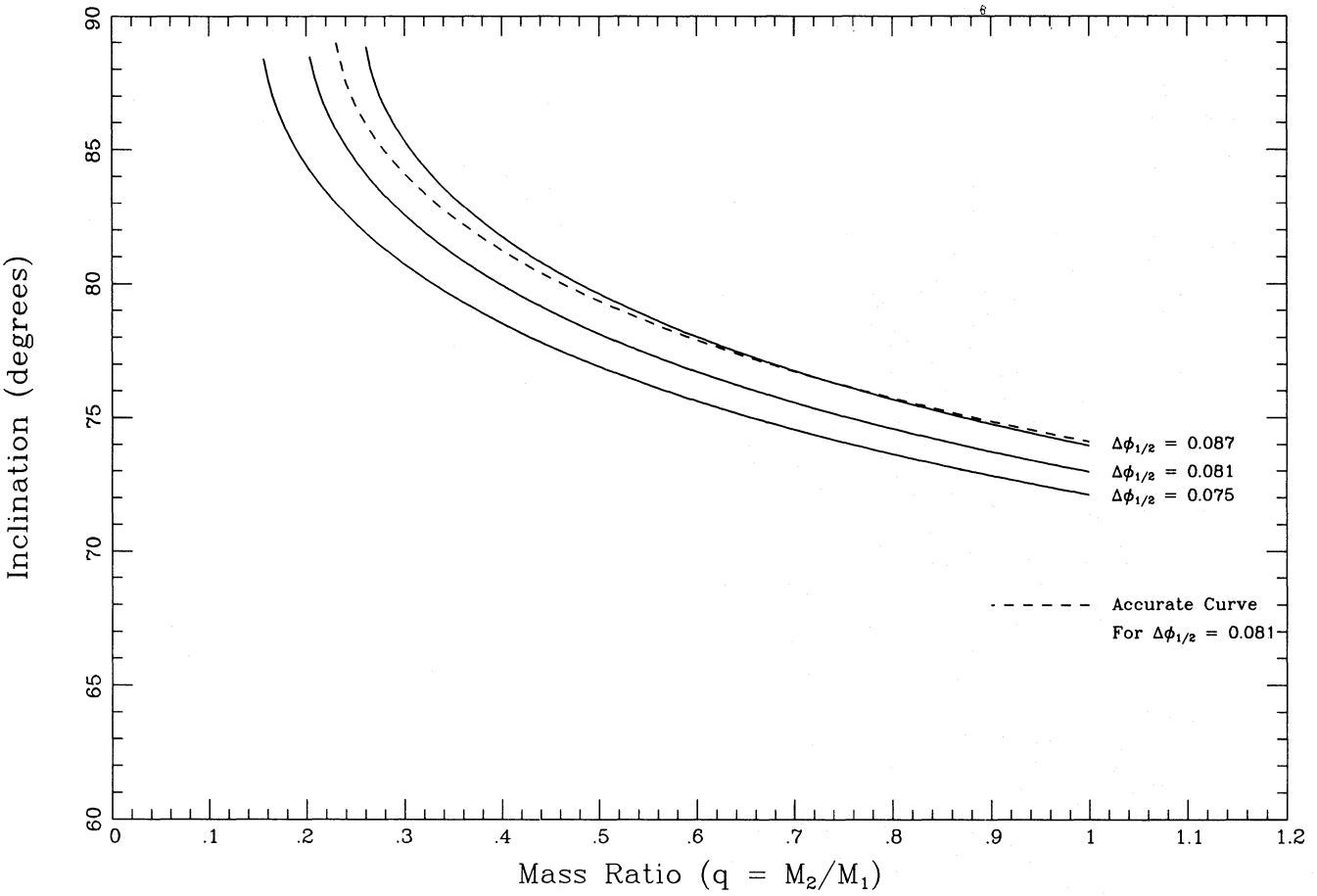

Figure 2. Orbital inclination as a function of mass ratio for three different values of the eclipse width ($\Delta\phi_{1/2} = 0.081 \pm 0.006$). The dashed line represents a more accurate determination of the inclination using a method similar to that of Horne *et al.* (1982).

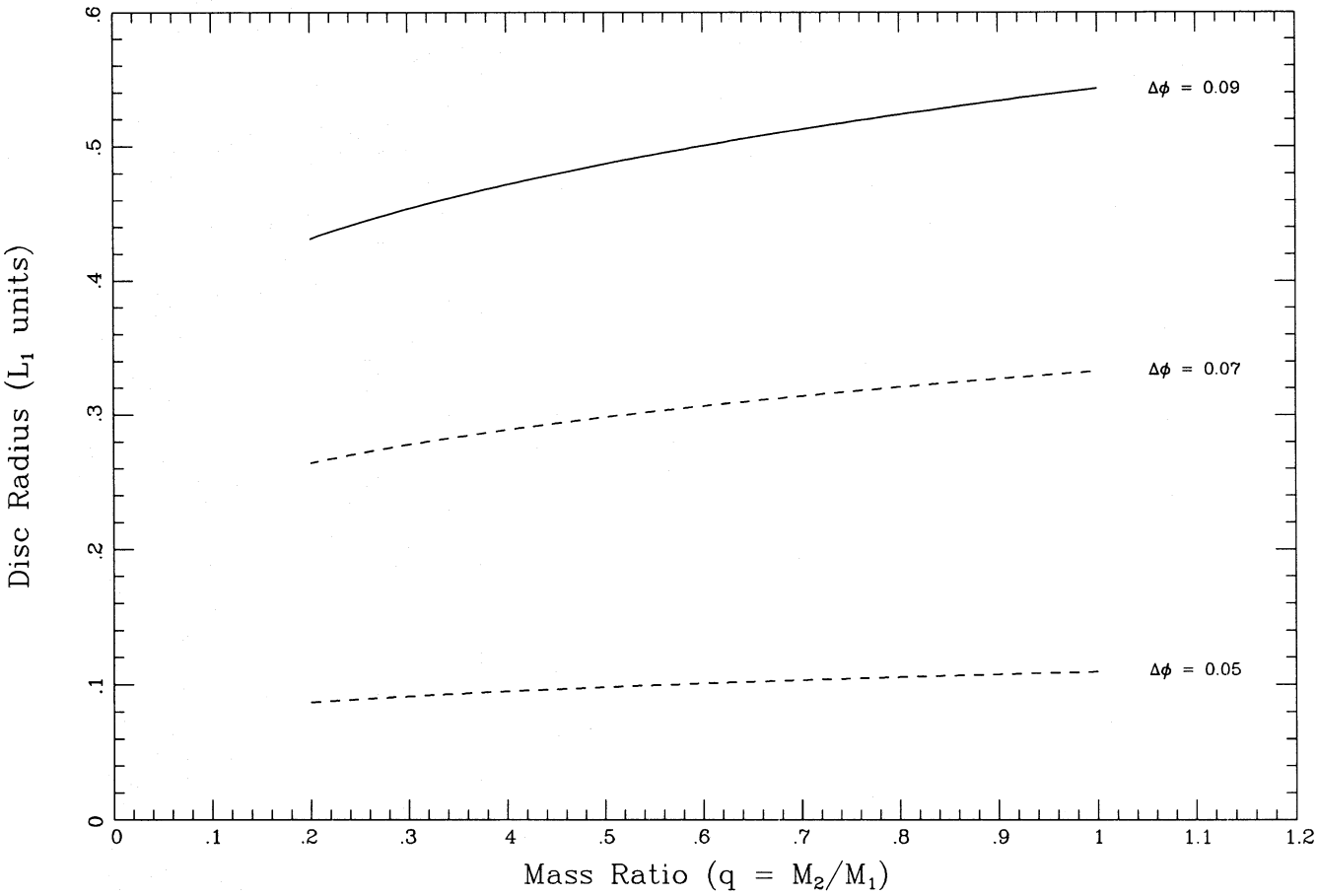

Figure 3. Accretion disc radius as a function of mass ratio for three different values of the eclipse width ($\Delta\phi = 0.07 \pm 0.02$). The dashed curves represent solutions where we would expect to see a total eclipse. The solid curve represents solutions where we would expect to see a partial eclipse.

eclipse (Fig. 7), with an eclipse width of $\Delta\phi = 0.07 \pm 0.02$, is *possibly* total, whereas the *R*-band eclipse (Fig. 1), with an eclipse width of $\Delta\phi = 0.08 \pm 0.02$, is almost definitely partial. This is as expected, given a canonical temperature distribution in the accretion disc (Bath & Pringle 1985).

By taking a representative value for the mass ratio of BH Lyn of $q = 0.41 \pm 0.26$ (see Section 3.2.5) and an eclipse width of $\Delta\phi = 0.07 \pm 0.02$, we find a disc radius (in the effective *B* band) of $R_D = 0.29 \pm 0.23\ L_1$ (where L_1 is the distance between the white dwarf and the inner Lagrangian point). Given the large uncertainty in the mass ratio and, more importantly, the difficulty in measuring $\Delta\phi$, this radius must be viewed with extreme caution (as reflected by the large error). However, it does appear that the disc in BH Lyn is small compared to other nova-like variables and dwarf novae (e.g. V1315 Aql: $R_D \simeq 0.66\ L_1$, Dhillon *et al.* 1991; IP Peg: $R_D \simeq 0.5\ L_1$, Marsh 1988), a result which will be discussed in greater detail in Section 4.

3.2 Spectroscopy

3.2.1 The spectrum

The average spectrum of BH Lyn from the 1990 January data, uncorrected for orbital motion and with eclipse spectra removed, is displayed in Fig. 4. In many respects, this

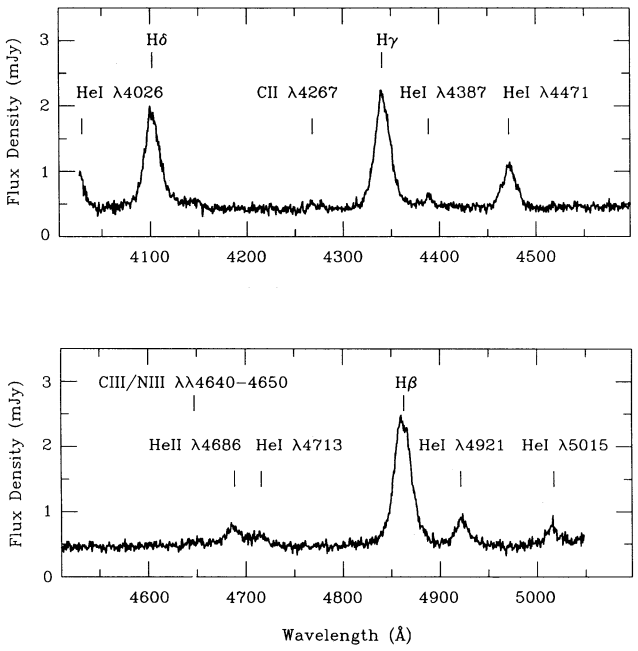

Figure 4. The average spectrum of BH Lyn in 1990 January, uncorrected for orbital motion and with primary eclipse spectra (phases −0.1 to 0.1) omitted.

spectrum is similar to those of a number of other eclipsing nova-like variables (e.g. V1315 Aql: Dhillon *et al.* 1991; DW UMa: Shafter *et al.* 1988; SW Sex: Honeycutt *et al.* 1986; PG 0027+260: Thorstensen *et al.* 1991b), exhibiting single-peaked Balmer and He I lines instead of the double-peaked profiles one would expect from a high-inclination accretion disc (see Horne & Marsh 1986). On the other hand, the high-excitation lines of He II λ4686 Å, C III/N III $\lambda\lambda$4640–4650 Å, C II 4267 Å and the numerous weak features in the continuum, which appear so prominently in objects such as V1315 Aql, are extremely faint in BH Lyn.

This latter result is contradicted by the blue 1991 April spectra presented in Fig. 5, which clearly show strong high-excitation features. Coupled to the fact that the continuum level in the 1991 April spectra is a factor of ~6 higher than in the 1990 January spectra and therefore approximately

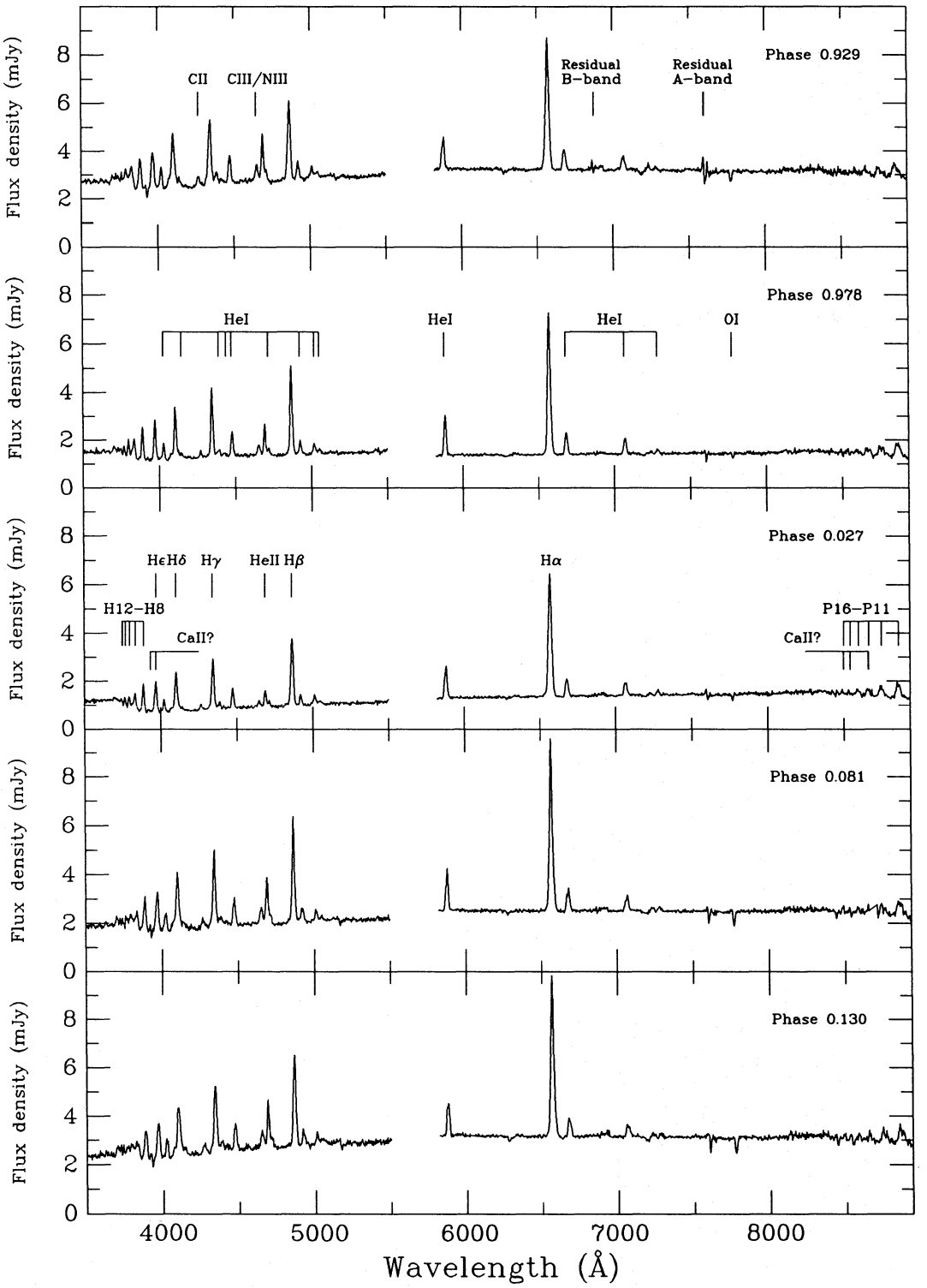

Figure 5. The 1991 April spectra of BH Lyn.

2 mag brighter than the 1990 January level of $V = 17.2 \pm 0.2$ [estimated from the average spectrum (Fig. 4) by extrapolation], we may conclude that we obtained the vast majority of our data during a low state. This conclusion is further supported by the brightness variations reported by Andronov *et al.* (1989). Thorstensen *et al.* (1991a), who observed BH Lyn just over 2 weeks after we did, reported a magnitude of $V = 16.9 \pm 0.2$, suggesting that they also obtained data either during or on the rise following a low state. There appear to be no spectral features from the secondary star (such as the $\lambda\lambda$8183.3, 8194.8-Å Na I doublet, Friend *et al.* 1988) in the red 1991 April spectra (Fig. 5), although O I λ7773-Å absorption from the accretion disc is visible.

In Table 3 we list fluxes, equivalent widths and velocity widths of several prominent lines measured from the 1990 January average spectrum (Fig. 4) and the phase-0.130 spectrum of the 1991 April data (Fig. 5). Although the line fluxes during 1991 April are higher than during 1990 January, the equivalent widths are lower, a result of the decreased continuum level during the low state.

3.2.2 *Emission-line variations*

We rebinned the three nights of spectra obtained during 1990 January on to a uniform wavelength scale and cast the data into 10 binary phase bins by averaging all the spectra falling into each bin. A multiple of 2 was then added to each spectrum in order to displace the data in the *y*-direction. The result is plotted in Fig. 6.

The line profile variations in the Balmer and He I lines are extremely complex and appear to be similar to those observed in BH Lyn by Thorstensen *et al.* (1991a) and in other eclipsing nova-like variables. The Hβ line is narrow and single-peaked, except during phase 0.5 when it shows a double-peaked structure. There is also a doubling of the line profile during phases 0.8 and 0.9. The line-doubling in Hγ, Hδ and He I is not so clear. The visual impression from Fig. 6 is that of one or more emission or absorption components superimposed on the line and moving relative to the line centre. As observed in V1315 Aql (Dhillon *et al.* 1991), the Balmer and He I lines remain single-peaked and are only partially eclipsed at phase 0. However, in the case of BH Lyn, the appearance of a partial eclipse is an artefact of the phase binning and the lines are actually deeply eclipsed at phase 0 (see Section 3.2.3). The weak high-excitation lines appear to be totally eclipsed at phase 0 [and the 1991 April spectra (Fig. 5) also show evidence of an eclipse of the high-excitation lines].

Table 3. Fluxes and velocity widths of prominent lines in BH Lyn, measured from the average spectrum of 1990 January and the phase-0.130 spectra (red and blue) of 1991 April.

	1990 January			
Line	Flux $\times 10^{-14}$ erg cm^{-2} s^{-1}	EW Å	FWHM km s^{-1}	FWZI km s^{-1}
Hβ	5.81 ± 0.04	94.3 ± 0.6	1300 ± 100	4000 ± 400
Hγ	5.65 ± 0.04	79.2 ± 0.5	1400 ± 100	4000 ± 400
Hδ	5.43 ± 0.05	69.2 ± 0.6	1400 ± 100	4000 ± 400
HeI λ4921	0.97 ± 0.04	16.2 ± 0.6	1100 ± 200	3000 ± 800
HeI λ4471	1.57 ± 0.03	22.6 ± 0.5	1200 ± 200	3000 ± 800
HeII λ4686	0.79 ± 0.03	12.1 ± 0.4	1200 ± 200	3000 ± 1000
	1991 April			
Line	Flux $\times 10^{-14}$ erg cm^{-2} s^{-1}	EW Å	FWHM km s^{-1}	FWZI km s^{-1}
Hα	11.49 ± 0.05	52.0 ± 0.2	1100 ± 100	4200 ± 400
Hβ	10.02 ± 0.13	27.8 ± 0.4	1200 ± 100	4000 ± 400
Hγ	8.68 ± 0.10	20.0 ± 0.2	1400 ± 100	3800 ± 400
Hδ	7.17 ± 0.09	15.2 ± 0.2	1600 ± 100	3800 ± 400
HeI λ7065	0.87 ± 0.05	4.6 ± 0.2	1200 ± 200	2000 ± 600
HeI λ6678	1.20 ± 0.04	5.6 ± 0.2	1000 ± 200	2200 ± 600
HeI λ5875	2.51 ± 0.04	9.0 ± 0.1	1000 ± 200	2500 ± 600
HeI λ4921	1.42 ± 0.12	4.0 ± 0.3	1300 ± 200	2500 ± 600
HeI λ4471	1.97 ± 0.10	4.7 ± 0.2	1100 ± 200	3000 ± 600
HeII λ4686	4.53 ± 0.10	11.8 ± 0.3	1000 ± 200	3000 ± 800
OI λ7771	−0.64 ± 0.05	−0.4 ± 0.3	600 ± 100	1600 ± 600

3.2.3 *The light curves*

We binned the 241 spectra obtained during 1990 January into 75 binary phase bins and fitted the continuum of each spectrum using a third-order polynomial fit. The flux in each line was then derived by summing all of the residual flux in a line after continuum subtraction. The five upper panels of Fig. 7 show the continuum light curve (in the range $\lambda\lambda$4150–4300 and 4500–4650 Å) and those of Hβ, Hγ, Hδ and He I λ4471 Å. The bottom panel in Fig. 7 shows the light curve of the wings of Hβ (-2000 to -500 and 500 to 2000 km s^{-1}) and the core of Hβ (between ± 500 km s^{-1}), where the data have been *uncorrected* for orbital motion.

The continuum light curve shows a deep, rounded eclipse, with a distinct hump before primary eclipse. An inspection of the data prior to phase-binning reveals that this feature is repeatable, which suggests that the origin of the hump is most likely due to the changing aspect of the bright-spot on the rim of the accretion disc, similar to the orbital hump often observed in dwarf novae (e.g. Z Cha, OY Car, IP Peg; Wood *et al.* 1986, 1989). The fact that an orbital hump is visible in BH Lyn, but absent in, for example, V1315 Aql (Dhillon *et al.* 1991) can be readily understood given the difference in disc radius. Following Rutten, van Paradijs & Tinbergen (1992), the ratio of the bright-spot luminosity to the disc luminosity ($L_{\rm spot}/L_{\rm disc}$) is approximately equal to the ratio of the white dwarf radius to the radial position of the bright spot ($R_{\rm wd}/R_{\rm spot}$). Given that BH Lyn has a relatively small accretion disc, we would expect the bright-spot to be more prominent.

In contrast to V1315 Aql (Dhillon *et al.* 1991), SW Sex (Honeycutt *et al.* 1986; Dhillon 1990), DW UMa (Shafter *et al.* 1988) and PG 0027+260 (Thorstensen *et al.* 1991b), BH Lyn exhibits Balmer lines which are as deeply eclipsed as the continuum at phase 0. It is interesting to note that the depth of the eclipse appears to increase as one travels up the Balmer series. The He I λ4471-Å line also appears to be totally eclipsed at phase 0. It is not clear whether the increase in Hα equivalent width during primary eclipse reported by Thorstensen *et al.* (1991a) contradicts these results, given the apparent dependence of eclipse depth on Balmer line order. However, the 1991 April data presented in Fig. 5 show that the Balmer lines are not as deeply eclipsed as the continuum (and the high-excitation lines), which suggests

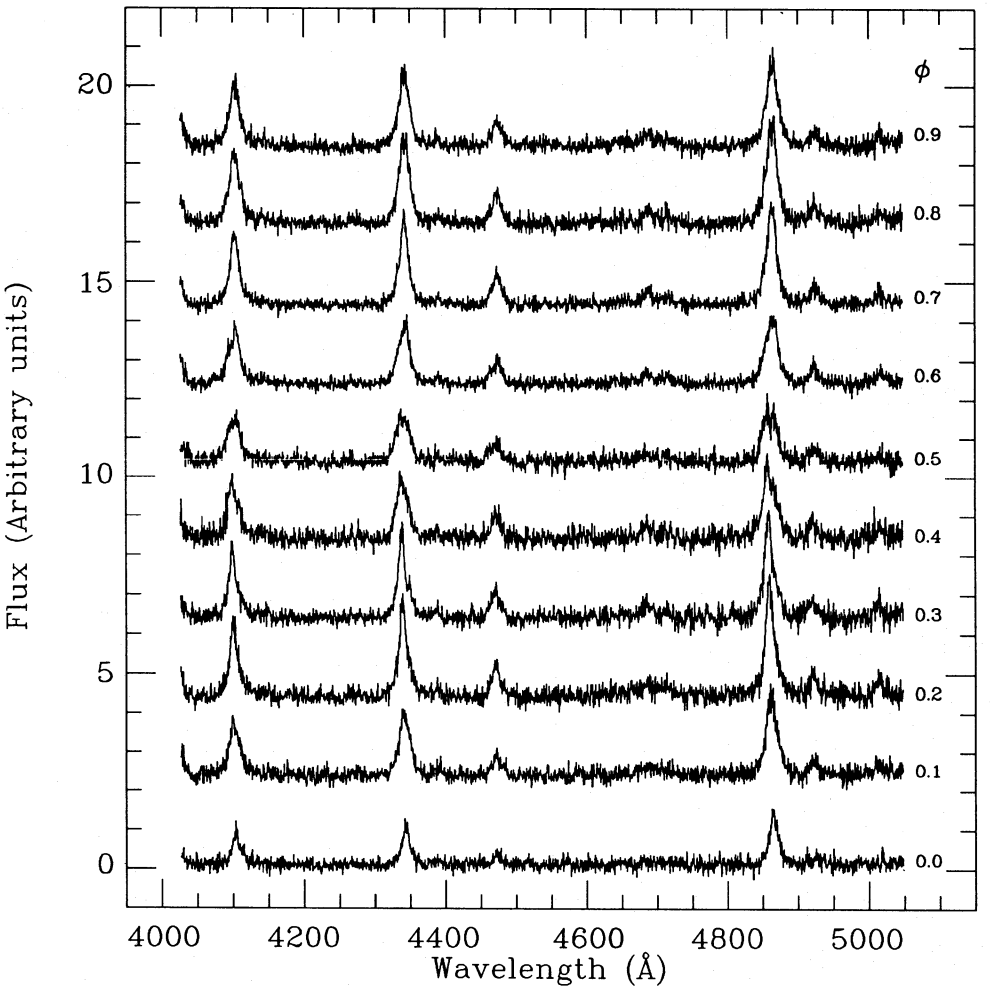

Figure 6. Orbital emission-line variations in BH Lyn. The data have been averaged into 10 binary phase bins with a multiple of 2 added to each spectrum in order to displace the data in the *y*-direction.

that, in its normal state, BH Lyn exhibits behaviour more typical of other eclipsing nova-like variables.

The low-state eclipse light curves of BH Lyn are generally different from those of other eclipsing nova-like variables. However, they do have one feature in common – the dip in Balmer line flux during phase 0.5. In V1315 Aql, this feature was stronger than the primary eclipse. The effect is smaller in BH Lyn and appears to decrease in strength as one travels up the Balmer series, thereby suggesting an absorption effect. Furthermore, the bottom panel in Fig. 7 indicates that the effect is most probably due to the absorption of *low*-velocity line emission. There is no evidence for a similar feature in the continuum light curve.

3.2.4 *Radial velocities*

We binned the 241 spectra obtained during 1990 January into 30 binary phase bins and subtracted the continuum of each spectrum using a third-order polynomial fit. The spectra were then binned on to a constant velocity interval (i.e. logarithmic) scale. In order to measure radial velocities, we used the double-Gaussian method of Schneider & Young (1980), since this technique is mainly sensitive to the motion of the line wings and should thus reflect the motion of the white dwarf with the highest reliability. The Gaussians were of width 200 km s^{-1} (σ) and we varied their separation a from 800 to 2600 km s^{-1}. We then fitted $V=\gamma-K\sin(\phi-\phi_0)$ to each set of measurements, omitting three points near primary eclipse with large measurement uncertainties. The results are listed in Table 4. Examples of the radial velocity curves obtained for Hβ, Hγ, Hδ and He I λ4471 Å using Gaussian separations of 1800 km s^{-1} are shown in Fig. 8.

As first noted by Thorstensen *et al.* (1991a), the radial velocity curves of BH Lyn appear very similar to those of other eclipsing nova-likes. In particular, Fig. 8 clearly shows that the spectroscopic conjunction of each line (i.e. superior conjunction of the emission-line source) occurs *after* photometric conjunction (i.e. photometric mid-eclipse). This phase shift implies an emission-line source trailing the accretion disc, such as the bright-spot, and has also been observed in V1315 Aql (Dhillon *et al.* 1991), DW UMa (Shafter *et al.* 1988), SW Sex (Honeycutt *et al.* 1986; Dhillon 1990) and PG 0027+260 (Thorstensen *et al.* 1991b). It is also interesting to note that the amplitudes of the radial velocity curves decrease as one travels up the Balmer series, although this could be an artefact of the apparent change in strength of the phase-0.5 absorption feature (see Section 3.2.6).

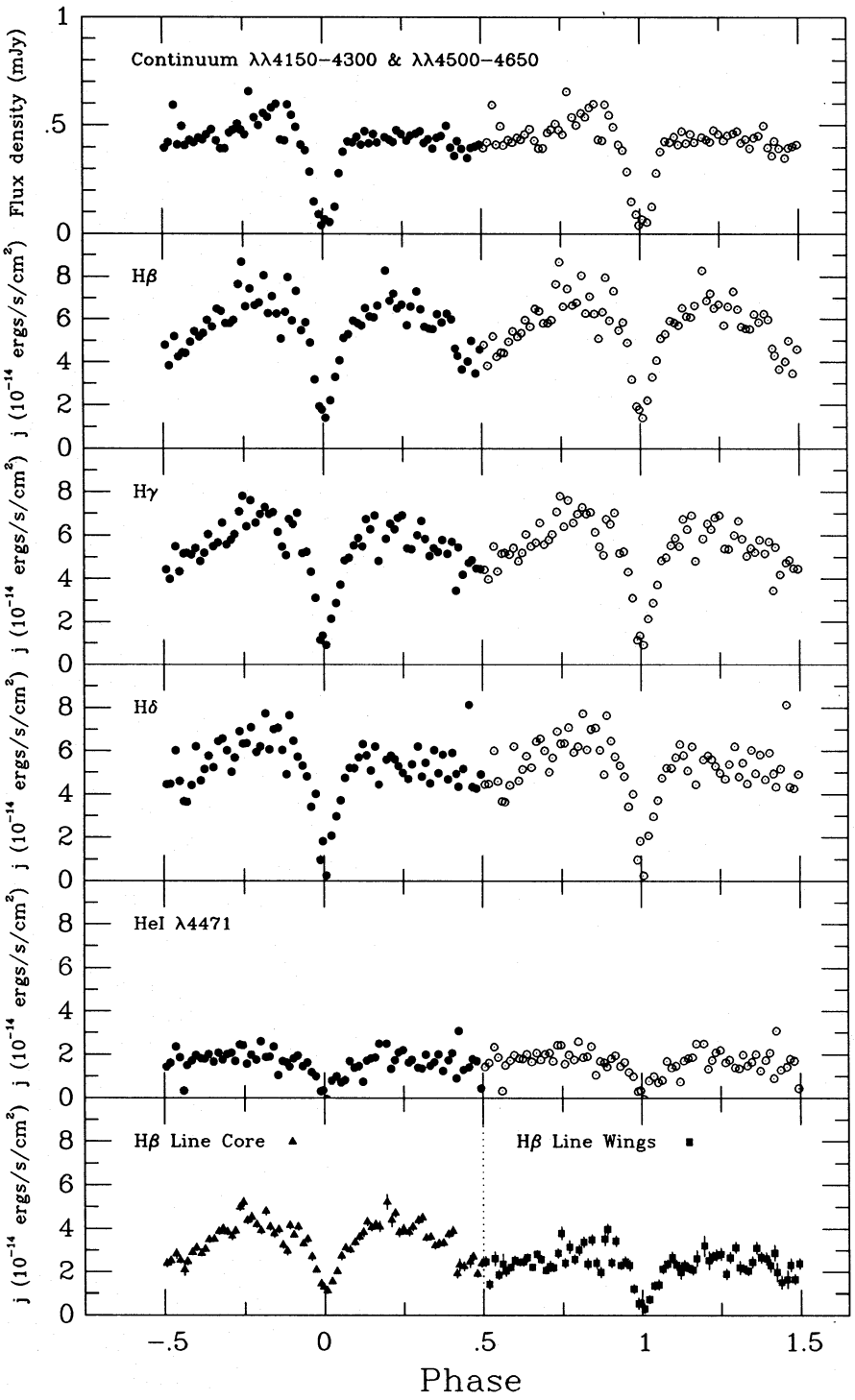

Figure 7. Upper five panels: continuum and line light curves of BH Lyn, computed by summing the flux between ±2000 km s^{-1}. The open circles represent points where the real data (closed circles) have been folded over. Bottom panel: light curve of the core (between ±500 km s^{-1}) and the wings (−2000 to −500 and 500 to 2000 km s^{-1}) of Hβ. The wing data have had a constant value of unity added to their phases in order to offset the data in the x-direction.

3.2.5 *System parameters*

The large phase shifts and peculiar line profiles observed in most eclipsing nova-likes indicate that any system parameter determinations are particularly unreliable. It appears from the results presented in Section 3.2.4 that BH Lyn will not be an exception to this rule. Following our analysis of V1315 Aql (Dhillon *et al.* 1991), we attempted to determine the radial velocity semi-amplitude of the white dwarf (K_W) in BH Lyn by applying the *diagnostic diagram* method of Shafter, Szkody & Thorstensen (1986) and the *light-centre* method of Marsh (1988).

Table 4. Radial velocity fits of BH Lyn. The parameters γ, K and ϕ_0 of the radial velocity fits for Hβ, Hγ, Hδ and He I λ4471 Å are presented for a series of different values of the separation a of the two Gaussians.

Line	a km s^{-1}	γ	σ_γ km s^{-1}	K	σ_K km s^{-1}	ϕ_o	σ_ϕ
Hβ	800	19	4	174	5	0.067	0.012
Hβ	1000	25	4	160	5	0.073	0.012
Hβ	1200	33	4	144	6	0.085	0.014
Hβ	1400	41	5	130	6	0.102	0.016
Hβ	1600	48	5	120	7	0.120	0.018
Hβ	1800	54	6	118	8	0.131	0.021
Hβ	2000	58	7	120	10	0.129	0.025
Hβ	2200	59	8	123	12	0.115	0.031
Hβ	2400	60	10	123	14	0.095	0.039
Hβ	2600	67	12	122	17	0.083	0.045
Hγ	800	27	4	147	5	0.058	0.015
Hγ	1000	35	4	137	6	0.072	0.015
Hγ	1200	44	5	122	6	0.087	0.017
Hγ	1400	50	5	112	7	0.102	0.019
Hγ	1600	53	5	108	7	0.108	0.022
Hγ	1800	54	6	103	8	0.105	0.025
Hγ	2000	55	6	97	9	0.097	0.030
Hγ	2200	53	7	90	10	0.087	0.038
Hγ	2400	49	9	80	13	0.075	0.052
Hγ	2600	54	11	73	15	0.087	0.073
Hδ	800	9	5	133	7	0.050	0.022
Hδ	1000	20	6	127	8	0.058	0.022
Hδ	1200	32	6	118	8	0.071	0.024
Hδ	1400	41	6	107	9	0.090	0.026
Hδ	1600	48	7	96	10	0.111	0.032
Hδ	1800	53	8	85	11	0.125	0.041
Hδ	2000	57	9	71	12	0.122	0.059
Hδ	2200	67	11	57	14	0.108	0.089
Hδ	2400	79	12	48	16	0.095	0.126
Hδ	2600	95	15	41	18	0.039	0.187
HeI λ4471	800	51	9	111	11	0.014	0.045
HeI λ4471	1000	53	10	101	13	0.060	0.053
HeI λ4471	1200	55	11	99	16	0.133	0.050
HeI λ4471	1400	54	11	105	17	0.176	0.043
HeI λ4471	1600	50	11	114	18	0.182	0.038
HeI λ4471	1800	51	12	123	20	0.182	0.037
HeI λ4471	2000	47	13	137	23	0.184	0.039
HeI λ4471	2200	54	17	130	26	0.178	0.055
HeI λ4471	2400	89	21	111	30	0.209	0.079
HeI λ4471	2600	90	21	90	32	0.227	0.098

The results of applying the light-centre method to BH Lyn are shown in Fig. 9. In order to make the interpretation of the figure easier, it should be noted that the error bars generally increase as the Gaussian separation increases. It is clear that not one of the emission lines exhibits the behaviour one would expect if there were some form of localized low-velocity distortion, such as from a bright-spot (e.g. IP Peg; Marsh 1988). In fact, it is difficult to reconcile the behaviour of the light centres with any known site of line emission in the canonical model. Obviously there is some other source of contaminating emission which cannot be accounted for with this method, a conclusion also reached in our study of V1315 Aql (Dhillon *et al.* 1991).

The diagnostic diagram for BH Lyn is presented in Fig. 10, based on the radial velocity fits to Hβ, Hγ, Hδ and He I λ4471 Å (Table 4). The curves generally show the same behaviour at all but the largest Gaussian separations. As noted by Thorstensen *et al.* (1991a), there is a steady increase in the phase shift as the Gaussian separation increases, which indicates that there is some source of contaminating emission other than the bright-spot. It is difficult to define an optimum Gaussian separation, since there is no distinct rise in fractional error (σ_K/K). Taking 1800 km s^{-1} as a best guess, the K-values for Hβ, Hγ, Hδ and He I λ4471 Å are 118, 103, 85 and 123 km s^{-1}, respectively (see Table 4 and Fig. 8). However, given the large scatter and the uncertainty in the origin of the low-excitation lines, we consider it extremely unwise to adopt any one of these K-values as K_W. A similar conclusion was reached by Thorstensen *et al.* (1991a), who derived a K-value of 196 km s^{-1} from their Hα radial velocity curves; we agree with their sentiment that it would be irresponsible to estimate the system parameters of BH Lyn using the emission-line radial velocity semi-amplitude. However, we did derive a representative value of the mass ratio for explicit use in Sections 3.1.3, 3.1.4 and 3.2.6, following the method outlined by Shafter (1984) and Dhillon *et al.* (1991). Adopting values of $K_W = 120 \pm 20$ km s^{-1}, $P = 0.15587507$ d, $b = 1.0$, $x = 0.88$ and $\Delta\phi_{1/2} = 0.081 \pm 0.006$, we obtain a mass ratio of $q = M_2/M_1 = 0.41 \pm 0.26$, where the error in q has been determined using a Monte Carlo simulation. However, we must stress that this value is *highly* uncertain and should only be taken as a *representative* figure.

3.2.6 *Doppler tomography*

Figs 11(a) and (b) show the observed data, Doppler maps and fitted data of the Hβ, Hγ, Hδ and He I λ4471-Å lines in BH Lyn. Before mapping, the 1990 January data (241 spectra) were binned into 50 binary phase bins, continuum-subtracted using a third-order polynomial fit, and then rebinned on to a constant velocity interval scale centred on the rest wavelengths of the lines.

The upper panels in Figs 11(a) and (b) present the observations in the form of trailed spectra. The middle panels contain the Doppler maps (see Marsh & Horne 1988 for details) constructed from the trailed spectra and the lower panels contain the predicted data computed from the maps. The blank strips in the fitted data correspond to eclipse data, which have been omitted in order to avoid the need for a relation between position and velocity in the map. The three crosses marked on the Doppler maps represent the centre of mass of the secondary (upper cross), the centre of mass of the system (middle cross) and the centre of mass of the primary star (lower cross). The secondary's Roche lobe and the predicted trajectory of the gas stream have been plotted using the representative mass ratio derived in Section 3.2.5. The series of small circles along the gas stream mark the distance from the white dwarf at intervals of $0.1L_1$, ranging from $1.0L_1$ at the red star to $0.3L_1$ at the left-most point. The grey scales start from zero in each panel and rise to the same upper level for each line, with the exception of the Doppler maps which have independently determined upper levels.

As observed in V1315 Aql (Dhillon *et al.* 1991), the most prominent feature in the trailed spectra of BH Lyn (Figs 11a and b, upper panels) is the strong absorption feature extending from phases 0.3–0.7 in all the lines. The core of this feature appears to shift from red to blue during these phases and its width appears to decrease as one travels up the

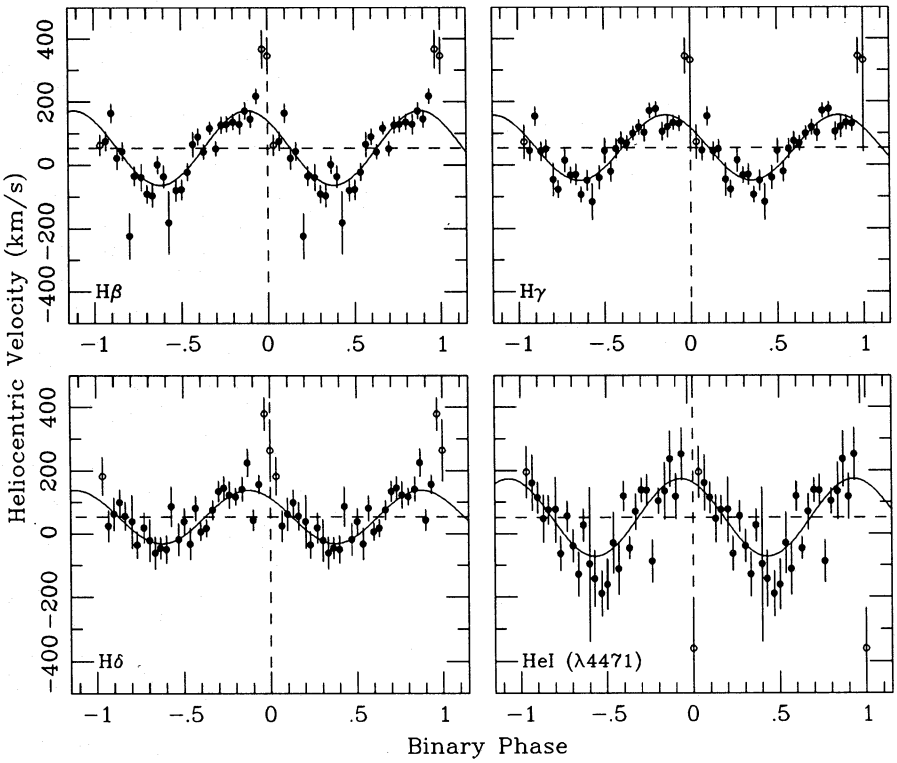

Figure 8. Radial velocity curves of the Hβ, Hγ, Hδ and He I λ4471-Å lines in BH Lyn, measured using a Gaussian separation of 1800 km s^{-1}. Points marked by open circles were not included in the radial velocity fits (due to measurement uncertainties during primary eclipse). The horizontal dashed lines represent the systemic (or γ) velocities.

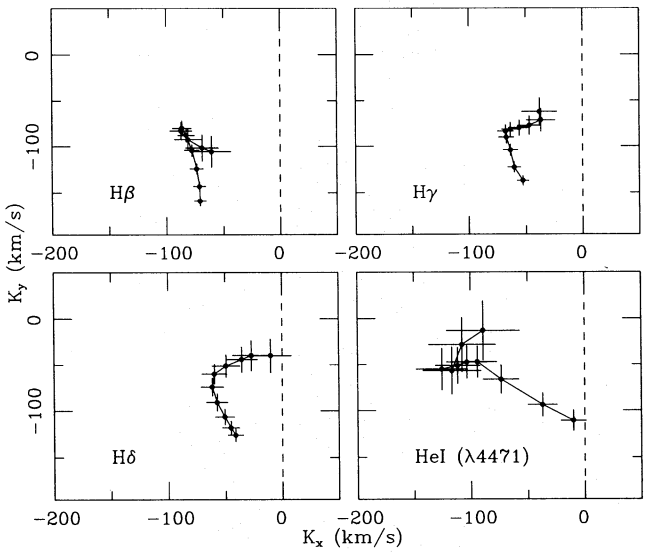

Figure 9. Light centres of the emission lines in BH Lyn deduced by plotting the results of the radial velocity fits to Hβ, Hγ, Hδ and He I λ4471 Å in velocity space.

Balmer series. A weak rotational disturbance and the absence of a total eclipse in the lines are apparent at phase 0. The orbital modulations of all the lines are very difficult to reconcile with the expected motion of the white dwarf in BH Lyn, a result confirmed by the preceding radial velocity analysis.

It is clear from the Doppler maps (Figs 11a and b, middle panels) that the strange emission-line behaviour observed in BH Lyn is not in any way associated with either the gas stream or the secondary star, even assuming extreme mass ratios. We may also conclude that, given the absence of a ring-like emission distribution (so clearly observed in, for example, IP Peg; Marsh & Horne 1990), there is no evidence for an accretion disc in Keplerian motion about the primary. Instead, the single-peaked line profiles, which appear to exhibit some form of sinusoidal radial velocity variation (Figs 11a and b, upper panels), are mapped in velocity space as emission peaks which have been smeared out due to the absorption during phase 0.5 (as evidenced by the poorly fitting computed data; Figs 11a and b, lower panels). The resulting Doppler maps are remarkably similar to those obtained for V1315 Aql (Dhillon *et al.* 1991) and SW Sex (Dhillon 1990), exhibiting line emission originating at a localized point with a velocity of $\sim(-200, -200)$ km s^{-1} for Hβ. As shown by the changing amplitudes of the radial velocity curves, the velocity of the peak intensity on the Doppler maps approaches that of the white dwarf as one travels up the Balmer series. This suggests that the higher order Balmer lines, which appear to be less affected by the phase-0.5 absorption, could prove to be more reliable indicators of K_W than the lower order lines. Nevertheless, given the uncertainty, we still believe that a system parameter determination is unjustifiable.

4 DISCUSSION

As discussed by Thorstensen *et al.* (1991a), it is clear that BH Lyn exhibits certain types of behaviour reminiscent of the cataclysmic variables V1315 Aql, DW UMa, SW Sex

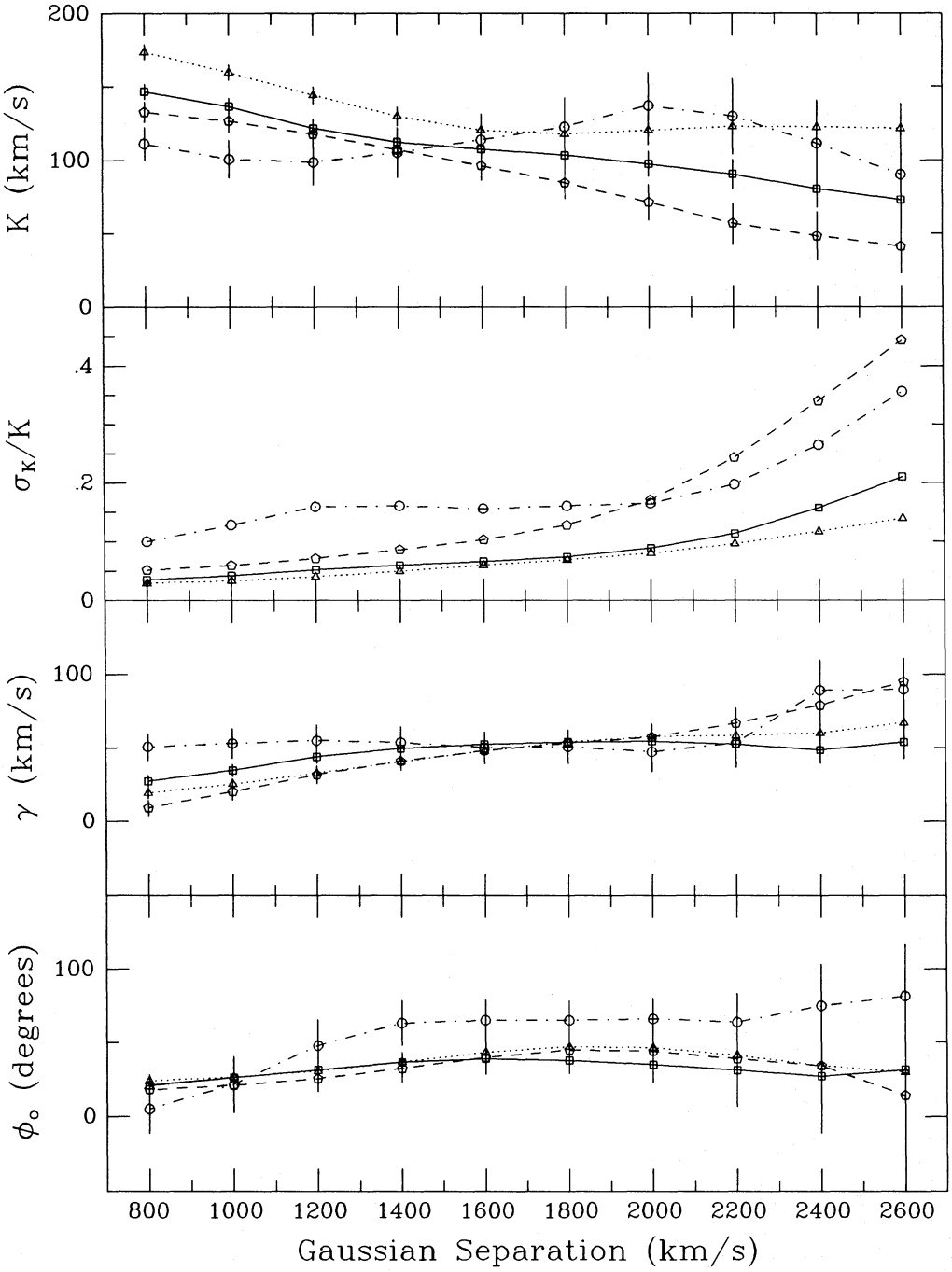

Figure 10. The diagnostic diagram for BH Lyn based on the radial velocity fits to Hβ (triangles connected by dotted lines), Hγ (squares connected by solid lines), Hδ (pentagons connected by dashed lines) and He I λ4471 Å (circles connected by dashed–dotted lines).

and PG 0027 + 260. All five objects show the following characteristics:

(i) eclipsing nova-like variables with periods of between 3.24 and 3.74 hr;

(ii) single-peaked Balmer and He I emission lines, which show absorption features around the inferior conjunction of the emission-line source, and

(iii) radial velocity curves with significant phase shifts relative to the expected radial velocity of the white dwarf.

Unfortunately, even with the above observational constraints, it has proved remarkably difficult to constrain the origin of the emission lines in these objects. A number of very different models have been proposed and have been discussed in detail by Dhillon *et al.* (1991). The two most likely candidates are an accretion disc wind or a magnetic accretion column. However, at a first glance, the basic constraints supporting both of these models appear to be violated by the 1990 January BH Lyn data, since

(i) the Balmer and He I low-excitation lines in BH Lyn are deeply eclipsed at phase 0, whereas they remain largely unaffected by primary eclipse in V1315 Aql, DW UMa, SW Sex and PG 0027 + 260;

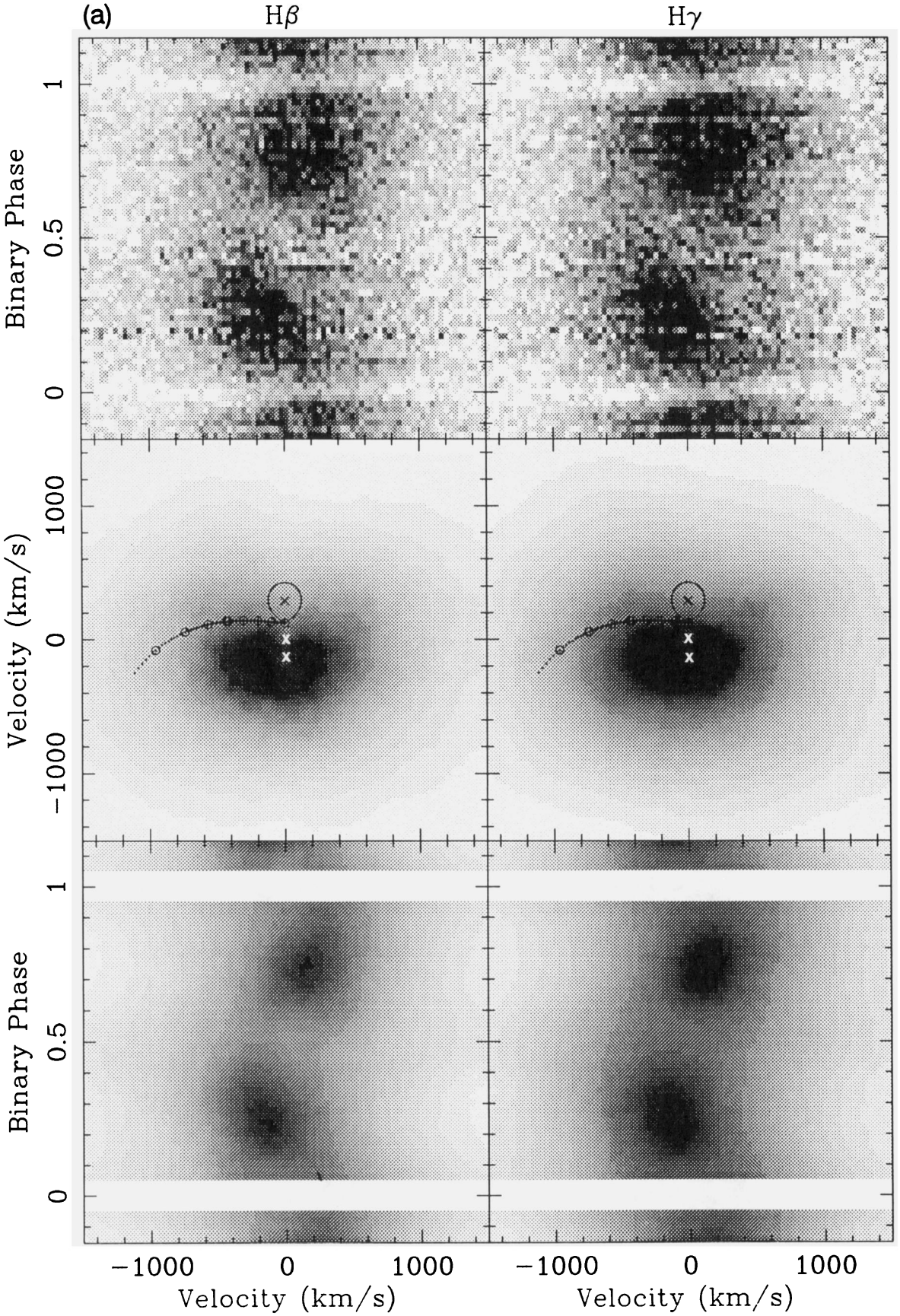

Figure 11. Trailed spectra of (a) Hβ and Hγ, and (b) Hδ and He I λ4471 Å in BH Lyn are displayed in the upper panels with the velocity relative to the line centre along the horizontal axis and orbital phase along the vertical axis. The central panels show the Doppler maps fitted to these data. The predicted position of the red star and path of the gas stream are marked. The three crosses in the map are, from top to bottom, the centre of mass of the red star, the system (at zero velocity) and the white dwarf. The lower panels show the fits computed from the maps; the gaps correspond to eclipse data which were omitted from the fit.

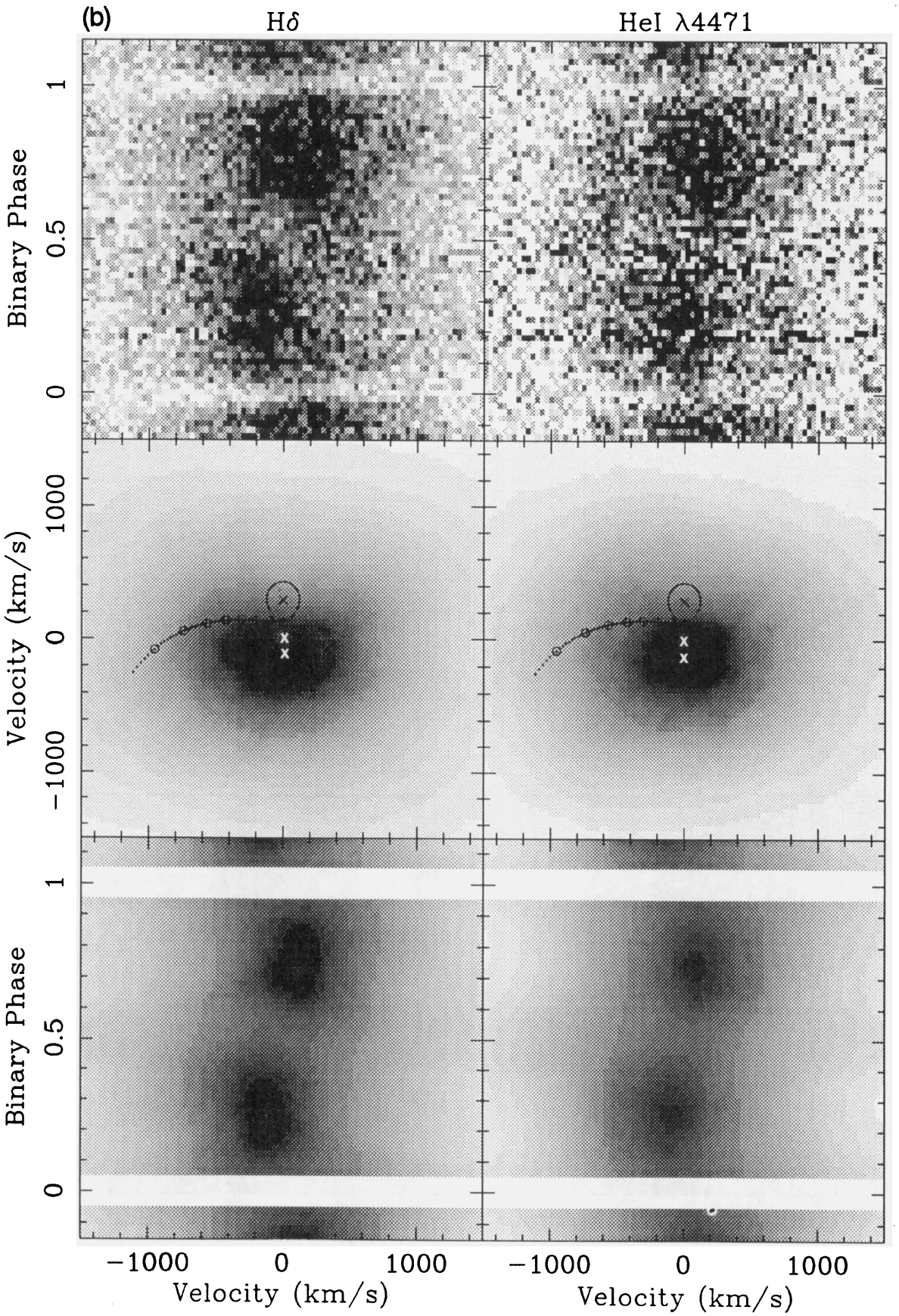

Figure 11 – *continued*

(ii) unlike V1315 Aql, DW UMa, SW Sex and PG 0027+260, the high-excitation lines of He II λ4686 Å and C III/N III λλ4640–4650 Å exhibited by BH Lyn are very weak, and

(iii) the width of the continuum eclipse in BH Lyn is very narrow compared to, for example, V1315 Aql.

How do these differences change our view of the origin of the emission-line variations? Given that the continuum and line eclipses are similar, it would seem reasonable to assume that both are formed in the accretion disc. The phase shifts and single-peaked lines can then be explained if there is strong line emission from a bright-spot overflow, as modelled by Lubow (1989). However, as with the other nova-like variables, this does not explain why the line wings are contaminated and why no *s*-wave effects are seen. It seems that the line formation is significantly more complicated than a simple disc plus localized bright-spot overflow model. Once again, we are led to the conclusion that some sort of accretion disc wind or magnetic accretion curtain model may be responsible, possibly interacting with a bright-spot overflow.

But how, then, within the context of these models, do we explain the obvious differences between BH Lyn, as displayed in the 1990 January spectra, and V1315 Aql, DW UMa, SW Sex and PG 0027+260? The most likely solution comes from the appearance of the 1991 April spectra of BH Lyn, which show strong high-excitation emission lines and a continuum level a factor of ~6 higher than in 1990 January. These observations imply that we observed BH Lyn during a low state in 1990 January. Such low states are not uncommon in nova-like variables; a low state in DW UMa was observed by Hessman (1990) and Dhillon (1990), during which mass accretion from the secondary was found to have effectively ceased. If we assume that the mass accretion rate has similarly decreased in BH Lyn [a hypothesis also supported by the appearance of high-excitation lines in the outburst spectra of dwarf novae (e.g. IP Peg, Marsh & Horne 1990), when the mass accretion rate is believed to increase by many orders of magnitude], we can account for many of the differences observed in the 1990 January spectra. For example, a lower mass accretion rate would reduce disc temperatures and thus render large parts of the outer disc optically thin in the continuum. This would have the effect of reducing the width of an eclipse at a given wavelength, as observed. In addition, since the Alfvén radius and the force driving the accretion disc wind both depend on the mass accretion rate, it seems likely that the observation of eclipses in the low-excitation lines is in accordance with the accretion disc wind and magnetic accretion curtain models, in the sense that line-emitting material would lie closer to the orbital plane and thus be eclipsed more deeply. Given the simple relation derived by Dhillon *et al.* (1991), we can constrain the height of the line emission above the plane of the disc in these models to be less than $\sim 0.25\ L_1$ (assuming the line is totally eclipsed, $i = 81.^{\circ}0$ and $q = 0.41$).

5 CONCLUSIONS

The detailed observational study of BH Lyn presented in this paper has confirmed that BH Lyn is yet another example of a growing number of eclipsing nova-like variables which exhibit homogeneous, repeatable and enigmatic behaviour. An unambiguous explanation of these phenomena still eludes us and further work, such as that reported by Rutten & Dhillon (1992) and Rutten *et al.* (1992), is essential if we are to be able to place these intriguing objects within the framework of the canonical model of cataclysmic variables.

ACKNOWLEDGMENTS

We are grateful to John Thorstensen for his comments on this paper. The spectra were reduced and analysed on the University of Sussex node of the SERC STARLINK network and the La Palma VAX 8300, using the PAMELA and RUBY software packages written by Keith Horne and TRM. The Isaac Newton Group of telescopes are operated on the island of La Palma by the Royal Greenwich Observatory in the Spanish Observatorio del Roque de los Muchachos of the Instituto de Astrofisica de Canarias. VSD is supported by a SERC Research Fellowship.

REFERENCES

Andronov, I. L., 1986. *Astr. Tsirk. No. 1418.*
Andronov, I. L., Kimeridze, G. N., Richter, G. A. & Smykov, V. P., 1989. *Inf. Bull. Var. Stars No. 3388.*
Bath, G. T. & Pringle, J. E., 1985. In: *Interacting Binary Stars,* p. 177, eds Pringle, J. E. & Wade, R. A., Cambridge University Press, Cambridge.
Dhillon, V. S., 1990. *D Phil thesis,* University of Sussex.
Dhillon, V. S., Marsh, T. R. & Jones, D. H. P., 1991. *Mon. Not. R. astr. Soc.,* **252,** 342.
Downes, R. A., Mateo, M., Szkody, P., Jenner, D. C. & Margon, B., 1986. *Astrophys. J.,* **301,** 240.
Eggleton, P. P., 1983. *Astrophys. J.,* **268,** 368.
Friend, M. T., Martin, J. S., Smith, R. C. & Jones, D. H. P., 1988. *Mon. Not. R. astr. Soc.,* **233,** 451.
Green, R. F., Schmidt, M. & Liebert, J., 1986. *Astrophys. J. Suppl.,* **61,** 305.
Green, R. F., Ferguson, D. H., Liebert, J. & Schmidt, M., 1982. *Publs astr. Soc. Pacif.,* **94,** 560.
Hessman, F. V., 1990. *IAU Circ. 4971.*
Honeycutt, R. K., Schlegel, E. M. & Kaitchuck, R. H., 1986. *Astrophys. J.,* **302,** 388.
Horne, K. & Marsh, T. R., 1986. *Mon. Not. R. astr. Soc.,* **218,** 761.
Horne, K., Lanning, H. H. & Gomer, R. H., 1982. *Astrophys. J.,* **252,** 681.
Jorden, A. R. & Fordham, J. L. A., 1986. *Q. J. R. astr. Soc.,* **27,** 166.
Kazarovets, E. V. & Samus, N. N., 1990. *Inf. Bull. Var. Stars No. 3530.*
Landolt, A. U., 1983. *Astr. J.,* **88,** 439.
Lubow, S. H., 1989. *Astrophys. J.,* **340,** 1064.
Marsh, T. R., 1988. *Mon. Not. R. astr. Soc.,* **231,** 1117.
Marsh, T. R., 1990. *Astrophys. J.,* **357,** 621.
Marsh, T. R. & Horne, K., 1988. *Mon. Not. R. astr. Soc.,* **235,** 269.
Marsh, T. R. & Horne, K., 1990. *Astrophys. J.,* **349,** 593.
Massey, P., Strobel, K., Barnes, J. V. & Anderson, E., 1988. *Astrophys. J.,* **328,** 315.
Oke, J. B. & Gunn, J. E., 1983. *Astrophys. J.,* **266,** 713.
Penning, W. R., Ferguson, D. H., McGraw, J. T., Liebert, J. & Green, R. F., 1984. *Astrophys. J.,* **276,** 233.
Richter, G. A., 1989. *Inf. Bull. Var. Stars No. 3287.*
Rutten, R. G. M. & Dhillon, V. S., 1992. *Astr. Astrophys.,* **253,** 139.
Rutten, R. G. M., van Paradijs, J. & Tinbergen, J., 1992. *Astr. Astrophys.,* in press.
Schneider, D. P. & Young, P. J., 1980. *Astrophys. J.,* **238,** 946.
Shafter, A. W., 1984. *Astr. J.,* **89,** 1555.

Shafter, A. W., Szkody, P. & Thorstensen, J. R., 1986. *Astrophys. J.*, **308,** 765.
Shafter, A. W., Hessman, F. V. & Zhang, E. H., 1988. *Astrophys. J.*, **327,** 248.
Thorstensen, J. R., Davis, M. K. & Ringwald, F. A., 1991a. *Astr. J.*, **102,** 683.
Thorstensen, J. R., Ringwald, F. A., Wade, R. A., Schmidt, G. D. & Norsworthy, J. E., 1991b. *Astr. J.*, **102,** 272.
Vogt, N., 1989. In: *Classical Novae,* p. 225, eds Bode, M. F. & Evans, A., Wiley, New York.
Wade, R. A. & Ward, M. J., 1985. In: *Interacting Binary Stars,* p. 129, eds Pringle, J. E. & Wade, R. A., Cambridge University Press, Cambridge.
Wood, J. H., Horne, K., Berriman, G., Wade, R. A., O'Donoghue, D. & Warner, B., 1986. *Mon. Not. R. astr. Soc.,* **219,** 629.
Wood, J. H. *et al.,* 1989. *Mon. Not. R. astr. Soc.,* **239,** 809.

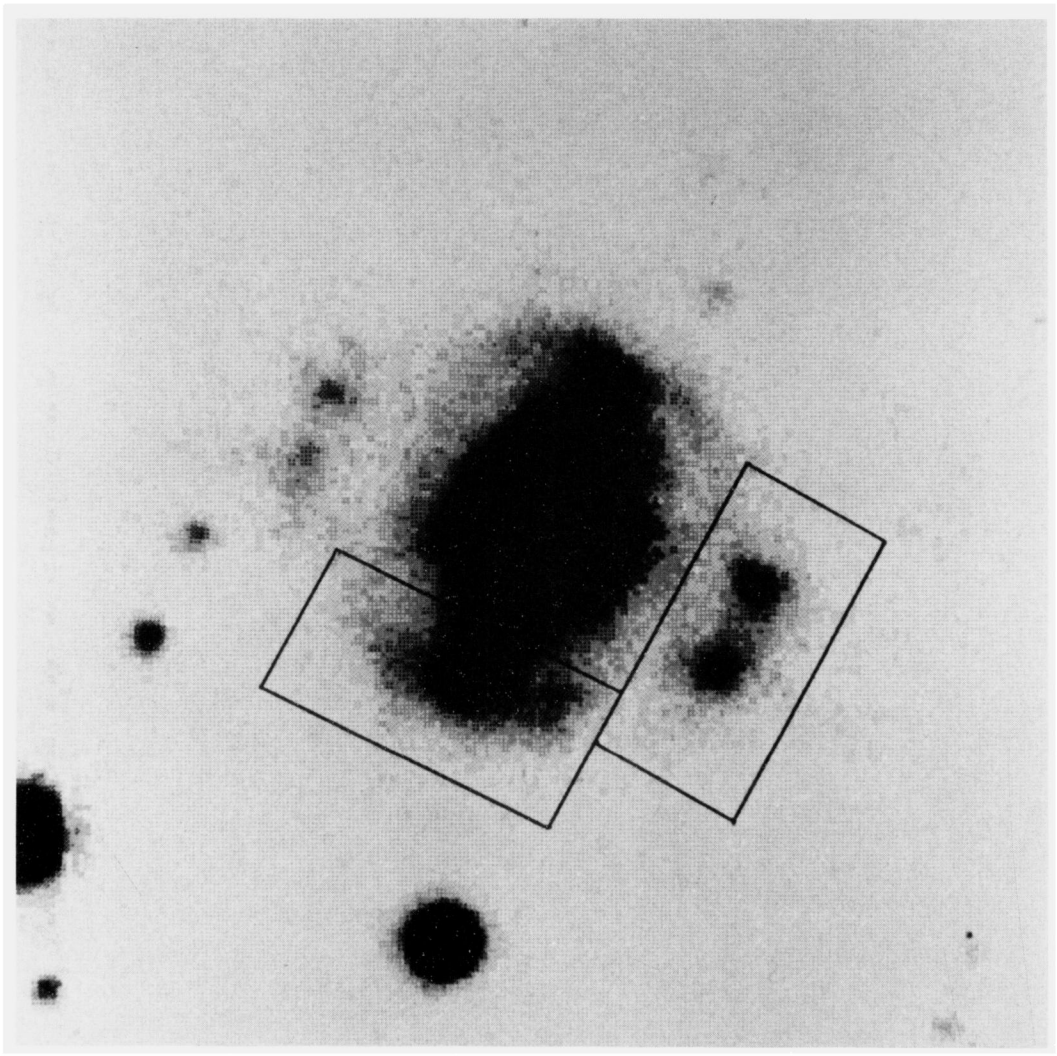

Plate 1. [N II]λ6584–Hα image of the RR Pic nebula obtained on the ESO 2.2-m telescope. The location of the *IUE* large aperture for each of the observations was as indicated. North up, east left.

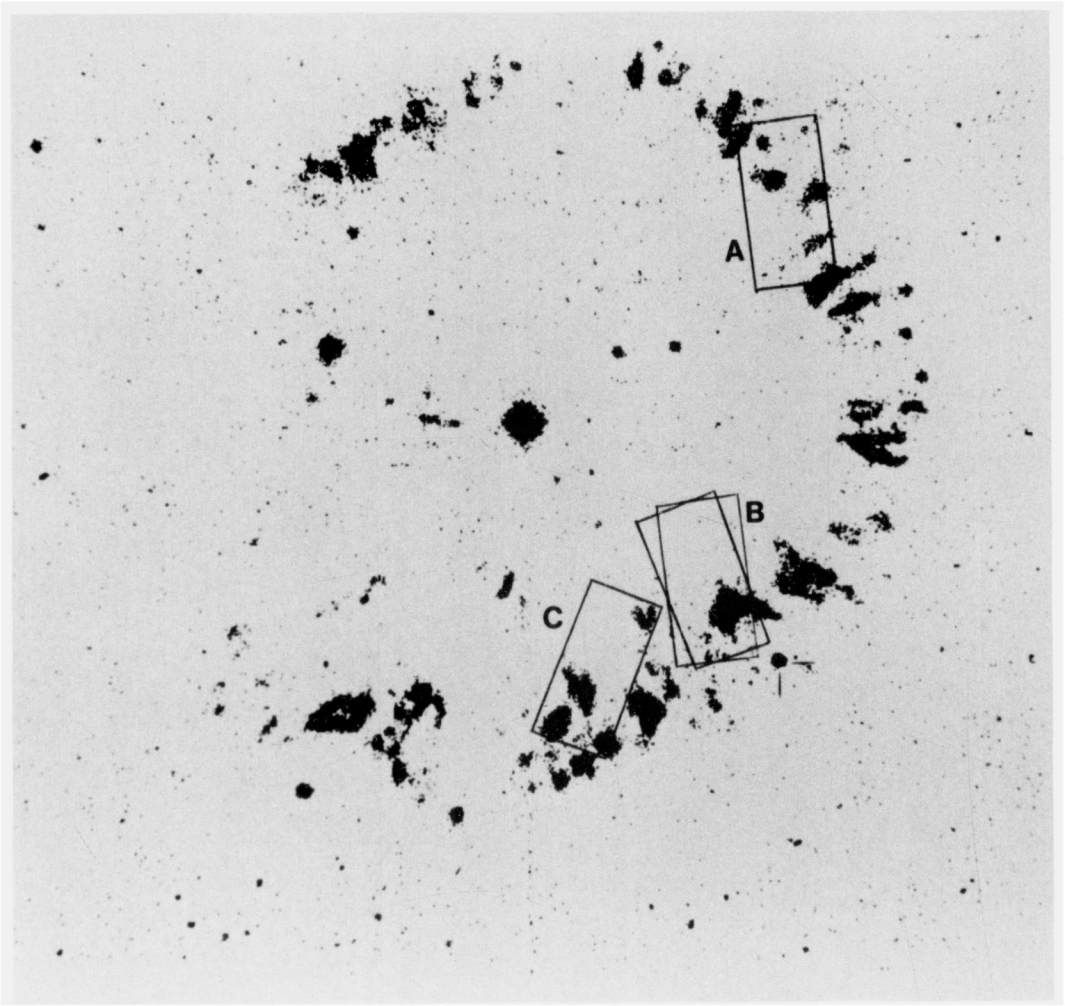

Plate 2. [N II]λ6584 image of the GK Per nebula obtained on 1991 December 25 with the Manchester Echelle Spectrograph in direct imaging mode on the Isaac Newton Telescope using an EEV CCD. The angular distance from GK Per to the marked reference star near location B is 43 arcsec; the radial expansion of the nebula is $\simeq 0.5$ arcsec yr^{-1}. The location of the *IUE* large aperture for each observation was as indicated. The letters correspond to those in Table 1. North up, east left.